

Kinetics of Plasma Particles and Electron Transport in the Current-Carrying Plasma Adjacent to an Evaporating and Electron Emitting Wall

Isak I. Beilis, *Senior Member, IEEE*

Invited Paper

Abstract—The paper reviews the vaporization phenomena at a target heated by heat flux from an adjacent plasma in vacuum and in low-pressure discharges. The kinetics of a nonequilibrium layer and the direct and returned mass fluxes formed in the vicinity of the target are described. The mechanism of cathode vaporization taking into account cathode electron emission in vacuum arcs is considered. It is shown that in vacuum arcs, the cathode electron beam relaxation region is an energetic zone which supports the generation of charged particles by atom ionization, balancing losses from ion motion towards the cathode and electron current. The mechanism of electron transport from the cathode to the plasma for cathode materials with strongly different thermal properties is considered. It is shown that the cathode electron current is controlled by a near-cathode space charge sheath whose structure depends on the thermo-physical properties of the cathode material. The potential structures has a large electric field at the cathode surface (like Cu), or a virtual cathode (W), or double plasma sheath (Hg), depending on the ratio of the electron emission flux to the vaporized atom flux, which in turn depends on the cathode material.

Index Terms—Ablative wall, current structure, current-carrying plasma, double sheath, electron emission, electron transport, nonequilibrium layer, plasma cathode, relaxation zone, vacuum, vacuum arc, vapor particle, vaporization phenomena, velocity distribution function, virtual cathode.

I. INTRODUCTION

ELECTRICAL current in vacuum can be maintained if neutral or charge particles are generated in the interelectrode gap. In a low-pressure gas, a high-current density discharge can be supported if the density of the charged particles in the near electrode area exceeds the ambient plasma density. Both in vacuum and low-pressure gas, the charged particles can be added by ionizing atoms emitted from the electrodes or walls. The classical examples of such discharges are the electrical arc in vacuum [1], [2] and discharges in low-pressure devices [3], [4].

Manuscript received September 30, 2005; revised December 6, 2005. This work was supported by a grant from the ISF founded by the Israel Academy of Sciences.

The author is with the Electrical Discharge and Plasma Laboratory, Department of Interdisciplinary Studies, Fleischman Faculty of Engineering, Tel Aviv University, Tel Aviv 69978, Israel (e-mail: beilis@eng.tau.ac.il).

Digital Object Identifier 10.1109/TPS.2006.873250

In ablative wall discharges (e.g., metallic electrode ablation in arcs [2], [5], Teflon ablation [3]), the velocity distribution function (VDF) is not in equilibrium in the region adjacent to the surface. A relaxation zone where the VDF of the evaporated atoms transforms to the equilibrium VDF is formed near the wall. The length of relaxation zone, named the Knudsen layer, is a few collisional mean free paths of the vapor particles. The hydrodynamic parameters (temperature, density, velocity) in the Knudsen layer establish the relationship between the equilibrium vapor pressure at the wall temperature and heavy particle pressure which is a result of plasma flow in the wall region. The phenomena are similar to those appearing during laser evaporation [6].

Considering current near the electrode, the following question must be addressed: *how is current continuity preserved from the highly conductive metallic electrode to the less conductive plasma near the electrode?* The electrical current is supported by the electrons in a metal and in the plasma. However, the electron densities in these media are vastly different. This leads to different mechanism of current continuity at the plasma interfaces with the anode and the cathode.

In many cases (depending on the gap geometry and discharge current), the whole anode surface operates as collector of the electrons ejected from the attached plasma. However, when the anode is relatively small, and in cases where the current cannot be collected by the entire anode surface, the anode plasma constricts and an *anode spot* appears. In this case, the constricted region forms an additional heat flux heating the anode and causing its evaporation at the level required for the process to be self-consistent [1]. The main problem of the anode region of a vacuum arc is the energy source for plasma generation. It was shown that the problem can be solved considering the Knudsen layer parameters and taking into account the ohmic energy dissipation in the spot plasma and in the region of plasma expansion from the spot [7].

At the cathode, only a small area of the surface contacts the constricted plasma region; electrons are emitted only from this area. Sufficient electrons and atoms are emitted for self-consistent current continuity. Experimentally, the contact between the plasma and the cathode in vacuum arcs appears as a bright spot named the *cathode spot* [1]. The time dependant phenomenology of cathode and anode spots as well as their parameters (current, velocity, erosion rate, etc.) were observed and described [1], [5].

Current continuity in the cathode region is more complicated. There are several phenomena such as atom evaporation, cathode electron emission, and a large electric field at the cathode surface due to the positive space charge of the ion flux to the surface. Therefore, a few relaxation zones are present for the flow of the atoms, ions, plasma electrons, and electron emitted from the cathode. A strong electric field accelerates the charged particles in the electric sheath near the cathode. Also, the difference in the temperature of various species and the bulk cathode temperature should be taken into account. A general formulation for ablation in the cathode region should be based on self-consistent consideration of these phenomena.

Thus, wall ablation in electrical discharges in essence is a transition between wall and the attached current-carrying plasma and the following questions should be considered.

- How does the VDF of the particles tend to equilibrium?
- What is the relation between the lengths of different particle relaxation zones?
- What is the relation between the plasma gasodynamic parameters in the Knudsen layer near the ablative wall and their equilibrium values?
- How does the rate of material evaporation into a current-carrying plasma differ from evaporation into vacuum?
- What is the mechanism of electron transport from the cathode to the plasma for cathode materials with strongly differing thermal properties?

Below, a review of evaporation phenomena in different plasma systems (Section II) and the state of kinetic vaporization theory (Section III) will be presented. The characteristic vacuum arc cathode spot parameters (Section IV) and the mechanism of current continuity for ablative wall-plasma transition in the cathode region with electron emission will be described (Section V). The characteristics of electron emission transport near different cathode materials (leading in some cases to a virtual or plasma cathode with a double sheath) will be discussed in Section VI and the reviewed results as well as the original calculations will be summarized in Section VII.

II. PLASMA SYSTEMS WITH ABLATIVE WALL

High intensity heat fluxes to walls or electrodes are generated in different plasma systems and these heat fluxes heat the wall and may lead to vaporization. Below, the plasma interaction with ablative walls in typical systems will be discussed.

Vacuum Arcs: Arcs are used in circuit breakers and in plasma systems used for tool coatings and thin film deposition [5]. The electrical current in vacuum can be conducted when the electrode vapor filled the interelectrode gap is ionized [1]. The electrodes are intensively heated by the high current density immediately adjacent to the electrode surfaces. The current is considerably constricted and hence the current density is very high at the cathode spot. The cathode spot is a region that includes the hot cathode surface which emits vapor and electrons and the dense plasma near the cathode from which the plasma jet expands into the ambient space. The electron current in the cathode plasma and in the plasma jet to the anode closes the electrical circuit. Usually, numerous cathode spots were observed for sufficiently large arc currents (e.g., 1 kA) [5]. The observation shows that cathode spots are very small luminous plasma regions that

move on the cathode surface. Spot types were classified [1], [5], [8], [9] according to the spot velocity V_s , spot lifetime t and spot current I . High-speed motion (10–100 m/s) and short lifetime ($< 10 \mu\text{s}$) are associated with type 1 spots. The type 1 spot current is relatively small, e.g., < 10 A. The spot velocity is lower when the cathode surface is cleaner. Therefore, it was defined the additional two subtypes of spot 1-I and 1-II for arc spot appeared before and after cleaning the cathode surface, respectively. Slow, ($V_s \sim 0.1$ m/s) spots with lifetimes of about $t = 100 \mu\text{s}$ and spot currents of about 10 A are defined as type 2 spots that preferably appear when a small amount of gas is present. Several spots can appear together on the cathode surface and this collection of spots is called a “group spot.” The group spot current for copper is in the range of $I = 100$ to 200 A. The periodic fluctuations of the spot brightness, on a nanosecond time scale, are associated with the lifetime of spot fragments. A fragment size of about $10 \mu\text{m}$ and current per fragment of about 10 A were found on *Cu* cathodes [9]. A small spot current about 0.1 A was observed by Kesaev on mercury and *Cu* film cathodes [10].

Ablative Plasma Accelerators: Typical ablative plasma accelerators include the pulsed plasma thruster (PPT) [3], capillary discharge [11], [12], electrothermal accelerators [13], and ablative railguns [14], [15]. Wall heating and evaporation forms ablated controlled discharges [16]. PPT is considered as an attractive propulsion option for orbit insertion, drag compensation and attitude control of small satellites [3], [17]. The PPT propellant (Teflon) is heated during the discharge by the plasma and ablates. The ablated vapor is ionized in the vicinity of the solid propellant and is accelerated by an electromagnetic force.

The rate of polyethylene ablation is necessary for determining a boundary condition used for calculating the ablative flow of plasma in a capillary channel [18]. In a railgun, the rail electrodes are heated by plasma column radiation and particle energy flux. The plasma is produced by electrode evaporation and ionization [19]. There the rate of electrode evaporation is determined the plasma density and the projectile acceleration.

MHD Power Generation: In this application, high speed and large enthalpy gas flows in a channel are slowed down by a crossed magnetic field, inducing an electric field. The ionization of the gas is enhanced by doping with low ionization energy atoms, such as potassium. The potassium also condenses from the gas on the cooled metallic electrode surfaces and then re-evaporates by the induced electrical discharges which are strongly constricted near the electrode [20]. It was shown that the plasma density in the constricted region reaches a level comparable to that in the cathode region of a vacuum arc and, therefore, the evaporation phenomena can be described similar to that in a vacuum cathode spot [20].

Unipolar Arcs in Tokamaks: The unipolar arc appears at electrically floating surfaces contacted by plasmas [21]. In contrast to usual bipolar arcs, the unipolar arc occurs at one electrode which serves both as cathode and anode. In a tokamak, this type of arc was observed as a hot spots [22], which leaves an erosion track at the isolated plate. The unipolar arc can introduce a large impurity flux into the core of tokamak plasma. The arc is initiated by negative charging of the floating surface to a large potential when a relatively hot plasma contacts the wall. The wall

potential reaches a few tens of volts with respect to the plasma and an intensive local heat flux causes wall evaporation.

Also, a unipolar arc can be generated in a low pressure plasmas and the surface phenomena (track size, erosion rate) depends on high-frequency power injected into the plasma [23]. The plasma generation in the hot spot of a unipolar arc is similar to that in the vacuum arc cathode spots and the erosion mass flow from the target in a tokamak can be studied by the mathematical model of the cathode erosion mass flow in vacuum arcs [1], [2]. The hot spot in a tokamak appears at the wall or at a film covered the wall. The erosion track, caused by arc spots on tungsten films covering a carbon substrate, was observed in experiments modeling unipolar arc phenomena in fusion plasmas [24].

Laser Action on Metals: In contrast to evaporation in a discharge, which can affect the plasma conductivity and the discharge current (dependent heat source), during moderate power laser radiation, the metal target is heated and vaporized by an independent heat source [6]. However, for sufficiently high-power laser radiation, power absorption in the plasma generated near the target must be taken into account. Plasma absorption reduces the power flux at the target surface on the one hand, while on the other hand, plasma interaction with the radiation and target [25], [26], as well as possible instabilities [27], must be taken into account.

III. KINETICS OF A CONDENSED MATERIAL VAPORIZATION IN A VACUUM

Langmuir [28] showed that the rate of evaporation W_L (atom/cm²/s) into vacuum from a surface is determined by the equilibrium (saturated) vapor pressure P as

$$W_L = \frac{P}{\sqrt{2\pi mkT_0}} \quad (1)$$

where m is the atom mass, k is Boltzmann's constant, and T_0 is the surface temperature. Equation (1) assumes that all evaporated atoms are evacuated from the surface into surrounding space and that none return. Equation (1) is applicable for relatively low temperatures when $P \leq 1$ torr [28]. Later, the evaporation of liquid mercury into vacuum was studied by Knudsen [29], who showed that for strong evaporation a kinetic treatment is required due to nonequilibrium effects, as shown schematically in Fig. 1. For higher surface temperatures, some atoms flow back to the surface due to rarefied collisions, and, therefore, the net rate of material evaporation is less than that given by (1). The saturated vapor pressure increases with the surface temperature and the dense vapor flow can be treated hydrodynamically. However, in the immediate vicinity of the surface, the collisions create a nonequilibrium layer of several mean free path lengths where the atoms are returned back to the surface. The particle distribution function f approaches equilibrium in this layer named *Knudsen layer* or *atom relaxation zone*. Collisions in the vapor relax the distribution function (DF) towards a Maxwellian form. Thus, two regions appear near the surface: 1) a nonequilibrium region with rare collisions and 2) a collision dominated region with hydrodynamic vapor flow. A kinetic approach was used to solve the Boltzmann equation to determine

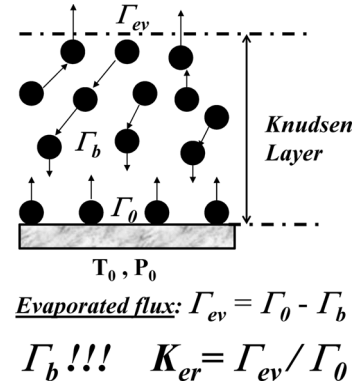


Fig. 1. Schematic diagram of rare atomic collisions in the Knudsen layer. Back flux Γ_b to the surface is generated at the length of Knudsen layer and Γ_0 is the direct atom flux in accordance with target temperature T_0 and saturated vapor pressure P_0 .

the flow parameters (density n , temperature T , and velocity v) in the nonequilibrium region. The parameters at the external boundary of the Knudsen layer determine the boundary condition describing the hydrodynamic flow along a path from the surface. In general, the Boltzmann equation is

$$\frac{\partial f}{\partial t} + \mathbf{v} \frac{\partial f}{\partial \mathbf{r}} = \left(\frac{df}{dt} \right)_{\text{col}} \quad (2)$$

where \mathbf{v} is the velocity vector, \mathbf{r} is a spatial coordinate, and f is the distribution function. Usually, (2) with the exact collision term $(df/dt)_{\text{col}}$ can only be solved for limited cases. Except of direct numerical simulation, the method of moments or modeling the collision term in (2) is used to analytical solve the kinetic problem. A given distribution function which differs only slightly from the local equilibrium distribution function f_0 is used. The collision term was modeled by Bhatnagar *et al.* (BGK); their approach is simplest for the present case of sharp variation of the vapor parameters near the wall [30]

$$\left(\frac{df}{dt} \right)_{\text{col}} = \frac{f_0 - f}{\tau} \quad (3)$$

This is called the relaxation model wherein a constant collision time τ is assumed. In most practical cases, the characteristic time of the hydrodynamic parameter set is smaller than the characteristic time of the heat flux change to the surface. Therefore, a steady state one-dimension problem was considered [6]

$$v \frac{\partial f}{\partial x} = \frac{f_0 - f}{\tau} \quad (4)$$

Boundary conditions

$$f_0 = n_0 \left(\frac{m}{\pi 2kT_0} \right)^{3/2} \exp \left[-\frac{mv^2}{2kT_0} \right]$$

$$v > 0 \text{ at } x = 0$$

$$f_\infty = n_\infty \left(\frac{m}{\pi 2kT_\infty} \right)^{3/2} \exp \left[-\frac{m}{2kT_\infty} ((v_x - u)^2 + v_y^2 + v_z^2) \right]$$

on the equilibrium side.

Anisimov considers the near surface nonequilibrium layer as a discontinuity surface in the hydrodynamic treatment of expanded vapor in laser-solid interactions [31]. His work was based on a previously developed approach to the shock wave problem or strong rarefaction wave problem and therefore bimodal distribution functions were used for the kinetic analysis [32]. In this case, the distribution function $f(x, v)$ within the nonequilibrium layer was approximated by the sum of two known terms before and after the discontinuity with coordinate-dependent coefficients $a(x)$

$$\begin{aligned} f(x, v) &= a(x)f_1(v) + [1 - a(x)]f_2(v) \\ f_1(v) &= f_0 \quad v > 0 \\ f_2(v) &= \beta f_\infty(v) \quad v < 0. \end{aligned}$$

The evaporated atoms have a half-Maxwellian DF (f_0) with the surface temperature and a given density [33], and this DF was served as boundary condition at the evaporated surface $x = 0$. At the external boundary (∞) of the Knudsen layer, the vapor particles are in equilibrium and therefore the full Maxwellian DF, $f_\infty(v)$ shifted by velocity u , was used. The relationship between the vapor parameters in the equilibrium and in the discontinuity region was obtained using the conservation of mass, momentum and energy and the conditions at the boundaries of the Knudsen layer: $a(0) = 1$ and $a(\infty) = 0$

Assuming sonic velocity at the external boundary $u = u_{sn}$ of the Knudsen layer, Anisimov [6], [31] obtained that the evaporated atom flux is about $0.82 W_L$. Fisher [34] solved the kinetic problem using the BGK approach and obtained that the rate of evaporation into an infinite half-space is about $0.85 W_L$. Thus, the obtained vapor flux is different from the flux W_L associated with equilibrium pressure calculated with surface temperature T_0 . The vapor flow regime with flow at the sonic velocity u_{sn} at the external boundary of the Knudsen layer, i.e., for condition $u = u_{sn}$ was named in the works of [35], [36] as the *free-flow* regime into vacuum. Bhatnagar *et al.* approach [30] was extended to the case of vaporizing molecules, taking into account their internal degrees of freedom [37], [38]. The Knudsen layer analysis was performed in order to predict the jump conditions across the layer for polyatomic gas as a function of the specific heat ratio γ and the Mach number M at the layer edge as parameters. It was shown that the jump of particle temperature and density increases with γ and M .

Electrode vaporization into plasma taking into account also the electron evaporation (emission) was treated kinetically by Beilis [35], [36], [39] (detailed below). The definition of an *nonfree (impeded)* plasma flow when $M < 1$ was introduced. The condition for impeded plasma flow was obtained. Using methods obtained earlier [31], [35], Teflon ablation in a discharge was calculated for known plasma density and temperature [40] and the analytical results were compared with direct simulation Monte Carlo (DSMC) [41] calculations. It was found that the thickness of the kinetic layer increases from a few particle mean free paths for small velocity ($M \ll 1$), up to about 10 mean free paths for evaporation with sound velocity at the outer boundary of the layer. This approach [35], [39]–[41] was used for analysis of the coupled phenomena between wall ablation and plasma flow in two types of PPTs. In one of them, the

discharge was between two electrodes across the Teflon propellant [42]. It was shown that the existence of two ablation modes with a velocity smaller than the local sound speed and a velocity close to the sound speed at the edge of nonequilibrium layer is determined by the current density in the acceleration region. In the other PPT, the propellant forms a coaxial Teflon cavity adjacent to a metallic anode and a ring cathode placed at the exit of the plasma flow [43]. The plasma flow in the cavity was investigated self-consistently taking into account the kinetics of the Teflon ablation. The mass ablation and impulse thrust as functions of the Teflon cavity length were calculated.

IV. CATHODE PLASMA AND ELECTRON BEAM RELAXATION ZONE

Let us consider the details of the ablation in the plasma adjacent to the ablative surface for vacuum arc cathode vaporization and electron emission. The transition characteristics between the cathode and the near cathode plasma will be described. The more simple case of nonemitted electrode was previously considered [7] by removing the effects of electron beam emission.

In this paper, as an example, a copper cathode will be considered. Let us discuss the typical plasma parameters in the near-cathode region. Within the framework of the vaporization model [1], [2], [44], the plasma consists of atoms, ions, and two groups of electrons—1) fast electrons in an emission beam and 2) slow plasma electrons. The ionized vapor near the cathode is characterized by a heavy particle density of $n_T \sim 10^{26} \text{ m}^{-3}$ with a degree of ionization of $\alpha = 0.1$ or more and an electron temperature of $T_e \sim 1 \text{ eV}$ and more, a slow plasma electron–electron mean free path of $L_{ee} \sim 0.01 \mu\text{m}$, and ion–ion and ion–atom mean free paths of $L_{ii} \sim L_{ia} \sim L_i \sim 0.01 \mu\text{m}$. The plasma is separated from the cathode surface by a space charge sheath (ballistic zone $\leq 0.01 \mu\text{m}$) with a potential drop U_c of about 15 V [10]. The cathode electron emission beam is accelerated in the ballistic zone, so that its electrons achieve a relatively large kinetic energy in comparison to the slow plasma electrons. The electron beam heats the slow plasma electrons in a relaxation zone L_b , as shown in Fig. 2. In general, the electron beam energy relaxes in several ways, namely by exciting plasma oscillations or by colliding with plasma particles [45]. An estimation showed that electron beam momentum and energy relaxation was due to collisions with plasma electrons [46]. Since the energy of electron beam exceeds the slow electron energy by an order of magnitude, the mean free path of accelerated beam electrons is two orders of magnitude larger than L_{ee} or L_i , i.e., the electron beam relaxation zone is about $L_b \sim 1 \mu\text{m}$.

Thus, inside the relatively large electron beam relaxation zone, a collision dominated plasma is formed. This fact is crucial for the model to be able to describe the cathode evaporation, using a hydrodynamic treatment in order to calculate the ion back flow to the cathode surface.

Since the spot radius is in the range of about $r_s = 10 - 100 \mu\text{m}$, the cathode evaporation problem can be considered in a one dimensional (1-D) approximation.

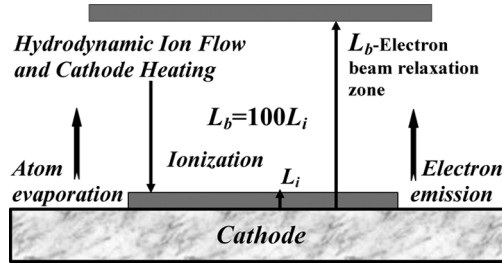


Fig. 2. Schematic model of the electron beam relaxation zone L_b and ion mean free path L_i in a vacuum arc cathode region illustrating the relative lengths and showing the ion flux to the cathode which can be calculated by hydrodynamic treatment of the ion flow.

V. KINETICS OF CATHODE VAPORIZATION

In general, to describe the kinetics of cathode vaporization, the following steady state system of equations in a one-dimension approximation should be solved

$$v \frac{\partial f_\alpha}{\partial x} + \frac{e}{m_\alpha} E(x) \frac{\partial f_\alpha}{\partial v} = S(f_\alpha) \quad (5)$$

$$\text{div} E = 4\pi e \left[\int f_i(v) dv - \int f_e(v) dv \right] \quad (6)$$

where indices $\alpha = e, i, a$ represent the electrons, ions and atoms respectively, and $E(x)$ is the electric field distribution in the near cathode region. The system (5), (6) is very complicated and, therefore, the following model was proposed taking into account the structure of the near cathode plasma and different characteristic relaxation zone lengths [1], [2], [35]. The near cathode vapor is a partially ionized gas that is separated from the cathode surface by an electrical sheath in which the charged particles are accelerated. The cathode is heated mainly by ions accelerated across the sheath and the collision dominated plasma is heated by the accelerated electron beam. In contrast to the simple model of only neutral atom evaporation by laser radiation [6], [31], there are two main characteristic discontinuity layers in the near cathode plasma—for the heavy particle and electron distribution functions.

Four characteristic boundaries can be distinguished in the near-cathode region, Fig. 3. The origin of the coordinate system is defined at the cathode surface, and the x direction coincides with the direction of the vapor flow. Boundary 1 is at the cathode surface at $x = 0$, boundary 2 is at the external boundary of space charge (ballistic) zone, boundary 3 is at a distance of the Knudsen layer length from the cathode surface for the heavy particles and plasma electrons, and boundary 4 is located at a distance equal to the electron emission beam relaxation length from the cathode surface. The gas parameters (density, velocity and temperature) at these boundaries are denoted as $n_{\alpha j}, u_{\alpha j}, T_{\alpha j}$, where indices $\alpha = e, i, a$ are the electrons, ions, atoms, respectively, and $j = 1, 2, 3, 4$ indicates the boundary number and n_{eo} and n_o are the equilibrium electron and heavy particle densities determined by the cathode surface temperature T_o .

The problem of cathode evaporation in a vacuum arc similarly to metal evaporation by laser radiation [6], [31] should be solved to determine the parameters only at the mentioned above control boundaries while their x dependence is not required, so that the problem reduces to integrating the equations which are ex-

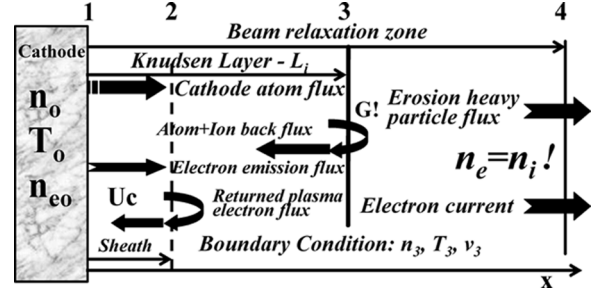


Fig. 3. Model of vacuum arc cathode evaporation. Structure of kinetic layers in the cathode current-carrying plasma.

pressed the conservation laws at the above particles and boundaries in following form:

$$\begin{aligned} \int f(x, v_\alpha) dv &= n_\alpha(x) \\ \int v_{\alpha x} f(x, \mathbf{v}_\alpha) d\mathbf{v}_\alpha &= n_\alpha(x) u_\alpha(x) \\ \frac{m}{2} \int [(v_{\alpha x} - u_\alpha)^2 + v_y^2 + v_z^2] f(x, \mathbf{v}_\alpha) d\mathbf{v}_\alpha &= \frac{3n_\alpha(x) k T_\alpha(x)}{2} \end{aligned} \quad (7)$$

where $f(x, \mathbf{v}_\alpha)$ is the velocity distribution function at the control boundaries, \mathbf{v}_α is the velocity vector, $v_{\alpha x}$ is the particle velocity component in the x direction and u_α is the velocity of the ionized vapor. Let us describe the VDF on all mentioned boundaries. The VDF is half-Maxwellian (positive velocity $v_{\alpha x}$) with the cathode temperature at the first boundary in accordance with particle emission from the cathode determined by evaporation for atoms [33] and for electrons [47]. The evaporated atoms are significantly ionized within one mean free path [44], therefore, the reverse flux consists of atom and ions, whose velocity distribution (negative velocity v_x) at boundary 1 can be approximated as shifted Maxwellian ones by the plasma parameters determined at this boundary from the problem solution [6].

At the external boundary 3 of the Knudsen layer, the heavy particles are in equilibrium. Therefore, the heavy particle distribution function is a shifted full Maxwellian with parameters $n_{\alpha 3}, u_{\alpha 3},$ and $T_{\alpha 3}$. For electrons, the VDF consists of a shifted full Maxwellian for the plasma electrons and a shifted half-Maxwellian for the electron emission beam. At boundary 4, the parameters of all particles are in equilibrium and, therefore, there the distribution functions are shifted full Maxwellians with parameters $n_{\alpha 4}, u_{\alpha 4}, T_{\alpha 4}$. Between the boundaries 1 and 2 is the space charge sheath. At boundary 2, the plasma electrons are returned, while the ions and emitted electrons are accelerated with energy eU_c . These effects determine the charged particle shift velocities and change the parameters of the VDF at boundary 2.

The velocity distribution function of the particles for $v_{\alpha x} < 0$ is denoted by $f_{\alpha j}^-$ and for $v_{\alpha x} > 0$ is by $f_{\alpha j}^+$, where

$$f_{\alpha j} = n_{\alpha j} \left(\frac{m_\alpha h_{\alpha j}}{\pi} \right)^{3/2} \times \exp \left[-m_\alpha h_{\alpha j} \left((v_{\alpha x} - u_{\alpha j})^2 + v_{\alpha y}^2 + v_{\alpha z}^2 \right) \right] \quad (8)$$

and where $h_{\alpha j} = (2kT_{\alpha j})^{-1}$, $v_{\alpha y}, v_{\alpha z}$ are the random particle velocity components in the y and z directions, m_α is the particle mass and k is the Boltzmann constant.

Next, the conditions at the boundaries are written

$$\begin{aligned} \text{At boundary 1 :} \quad & f_{\alpha 1} = f_{o\alpha 1}^+ + f_{\alpha 1}^-, \quad f_{oi 1}^+ = 0 \\ \text{At boundaries 3 and 4 :} \quad & f_{\alpha j} = f_{\alpha j}^+ + f_{\alpha j}^-, \quad j = 3, 4. \end{aligned}$$

In contrast to boundary 3, at boundary 4, the electron beam disappears and then the electron current is defined only by the electrical conductivity of the plasma (in essence, boundary 4 serves as the boundary for the electron Knudsen layer). Further, the problem is reduced to obtaining a system of equations from the conservation laws (7) taking into account the momentum and energy change due to the electric field in the space charge layer and the elastic and nonelastic collisions. Within the Knudsen layer, and hence at boundaries 1–3, the conservation laws (7), –(8) produce 18 equations. This system includes two equations for densities, four equations of mass continuity, and four equations for the momentum and energy (for heavy particles and electrons) at boundaries 1–2, as well as eight such equations at boundaries 2–3. However, at each boundary and for each particle, there are 28 unknowns (including the cathode potential drop) that follow: $n_{\alpha j}$, $T_{\alpha j}$, $v_{\alpha j}$, U_c .

The number of unknowns can be reduced to the number of equations taking into account the following conditions. Since the space charge layer thickness is much less than the Knudsen layer thickness, we have two quasi-neutrality conditions $n_{ej} = n_{ij}$ ($j = 2, 3$), assuming single ionised ions [44]. The mean free paths for ion–ion and ion–atom collisions are equal and that the effective momentum and energy relaxation lengths for heavy particles is determined by ion–ion collisions and is about one mean free path. Therefore, it can be assumed that $T_{ij} = T_{aj}$ ($j = 1, 2, 3$) and $v_{ij} = v_{aj}$ ($j = 3$). It should be noted that at boundary 2 the ion velocity is determined by the condition at the sheath-plasma interface (like Bohm condition) and at boundary 1 the ions are accelerated towards the cathode in the space charge layer, reaching a velocity of $v_c = (eU_c/m)^{1/2}$. This velocity is used as the shifted velocity for the ion distribution function at boundary 1. Finally, if the ionization-recombination length and plasma velocity are small in comparison to the length of the relaxation zone and to the thermal velocity, respectively, then at boundary 4 Saha's equation is fulfilled [44], i.e., $n_{e4} = n_{es}$, where n_{es} is the equilibrium electron density. In this case, an additional diffusion equation [44] determines the ion density at boundary 3, closing the above system of equations.

In order to determine the equilibrium parameters (n_{eo}, n_o) at the cathode surface, it is necessary to supplement the kinetic equations with equations for emission of electrons and heavy particles from the cathode, as well as with equation for the electric field (E) at the surface and the cathode energy balance (T_o) [2], [44]. The electron energy balance is determined by energy influx from the emitted electrons and energy dissipated by atom ionization, convective transport by the electric current, and ion outflow in the relaxation zone. In this formulation, the current per spot is a given parameter while the cathode and plasma parameters at the mentioned boundaries including the cathode potential drop can be determined as a part of the problem. The rate of mass flow of the ionized vapor G could be obtained by

$$G = mn_3v_3, \quad m = m_i = m_a, \quad n_3 = n_{a3} + n_{i3}. \quad (9)$$

Also, the plasma flow is divided into two basic regions, kinetic before boundary 3, and hydrodynamic after boundary 3. As results of the kinetic solution, the relation between the equilibrium parameters of n_{eo}, n_o, T_o , and the nonequilibrium plasma parameters at boundary 3 can be obtained (see below). Therefore, the plasma parameters at boundary 3 serve as boundary conditions for hydrodynamic equations of mass, momentum and energy in the expanded plasma jet. The details of the very bulky full system of equations can be found elsewhere [2], [35], [44], [46]. Examples of typical calculations as well as new calculated results will be present below showing the role of beam relaxation zone and sheath structure in cathode current continuity with different cathode materials.

VI. CALCULATION RESULTS

The saturated electron emission flux can be compared with the saturated vapor flux for different materials, according to their thermo-physical properties. The materials can be categorized into three classes for this comparison: 1) those with intermediate properties, e.g., Cu , 2) refractory materials with high values, e.g., W or 3) volatile materials with low values, e.g., Hg [1], [2]. The cathode materials can also be characterized by the ratio of the electron emission energy to the atom evaporation energy χ which can be related, respectively, to the mentioned classes as 1) $\chi \sim 1$, 2) $\chi < 1$, and 3) $\chi \gg 1$. It was shown [2] that for these materials, the plasma-cathode transition region has different structures and, therefore, different potential distributions and the electric fields near the cathode in electron beam relaxation zone. The electric field at the cathode surface is one of important parameters which control the current continuity in the cathode region [1], [2]. Let us consider the self-consistent calculation for each above mentioned case.

Intermediate Materials: The typical cathode materials with intermediate thermophysical properties include Cu, Ti, Al , and Ag , as well as graphite. For these materials, the solution of above mentioned system of equations can be obtained using the model presented here [2]. In the calculation below, Cu, Ti , and C cathodes are considered and the evaporated mass flow results are presented. In all calculations, the spot current, in the range $I = 1 - 20$ A, and the spot life time t , in the range from $0.1 \mu s$ to steady state, were used as parameters. The calculation showed that the electric field at the cathode surface is relatively large (~ 10 MV/cm) and the cathode electrons are emitted thermoionically, enhanced by the Shottky effect due to the large electric field.

The fraction of cathode mass loss $K_{er} = G/W_L$, the normalized plasma velocity $b_3 = m^{1/2}V_3/(2kT_3)^{1/2}$, the cathode erosion rate normalized by current $G_k = \pi r_s^2 G/I$, and the heavy particle density $n_{30} = n_3/n_0$ at external edge of the Knudsen layer (boundary 3) normalized by the saturated vapor density were obtained as functions of the spot current I [see Figs. 4(a)–7(a)] and life time t , [see Figs. 4(b)–7(b)]. The dependencies on spot current I were calculated for the steady state case and the dependencies on t were calculated for $I = 5$ A. It is shown that K_{er}, b_3, G_k increase and n_{30} decreases with spot current and life time. The mentioned time dependencies for Cu and C are similar and they are significantly different than for

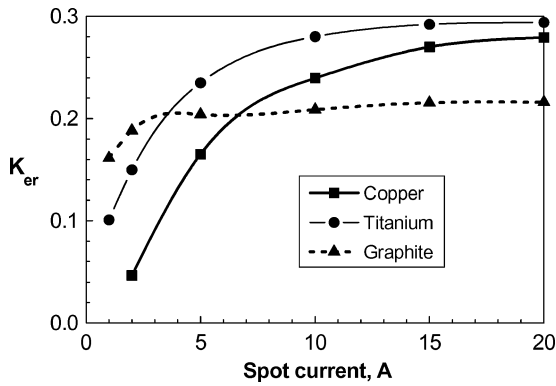


Fig. 4a. Steady state cathode evaporation fraction as functions of spot current.

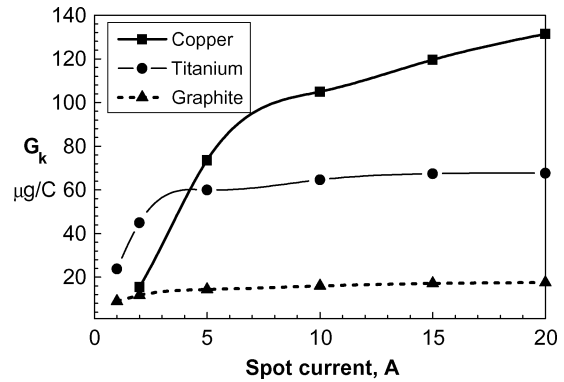


Fig. 6a. Steady state cathode erosion rates normalized by the spot current as functions of the spot current.

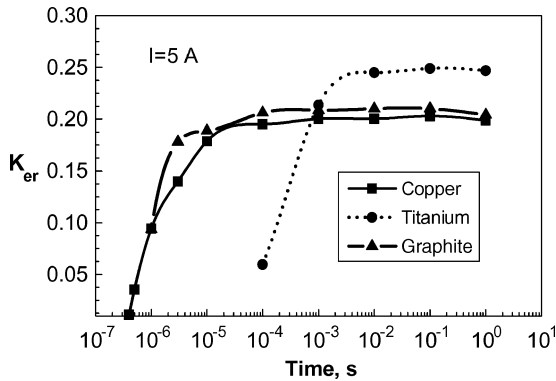


Fig. 4b. Time dependence of the cathode evaporation fraction.

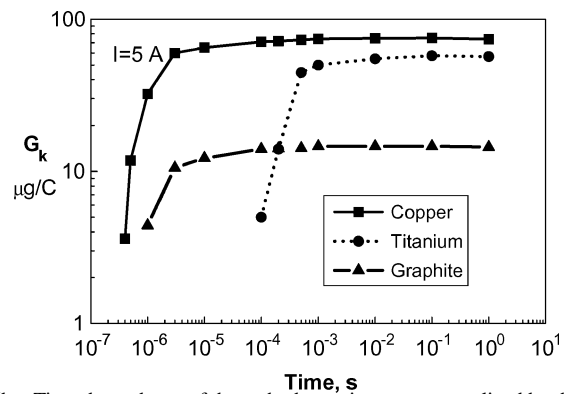


Fig. 6b. Time dependence of the cathode erosion rates normalized by the spot current.

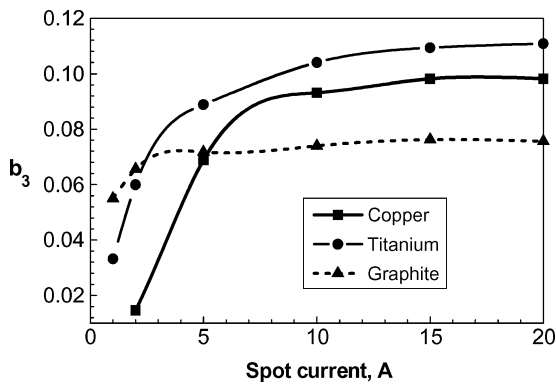


Fig. 5a. Steady state normalized plasma velocity at the external boundary of the Knudsen layer as functions of the spot current.

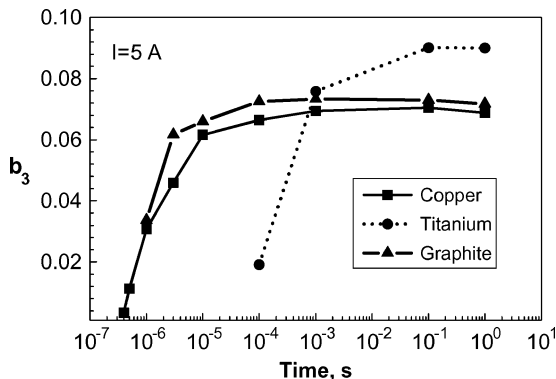


Fig. 5b. Time dependence of the normalized plasma velocity at the external boundary of the Knudsen layer.

Ti. The main change of the spot parameters with spot life time occurs up to about 10 μs for *Cu* and *C* and up to 1 ms for *Ti*.

The steady state cathode erosion rate for *Cu* is close to *Ti* and both are significantly larger than for graphite [Fig. 6(a)]. The main change of the spot parameters with spot current is up to about 10–15 A for *Cu* and *Ti* and up to 5 A for *C*. However, the character of the G_k dependence on I for *Ti* is close to that for *C* but they differ greatly in their absolute values [Fig. 6(b)].

Refractory Materials: The problem of current continuity in vacuum arcs with refractory cathodes stems from the thermophysical properties of refractory materials, leading to a large electron emission to atom evaporation rate ratio (~ 10) for a wide range of cathode temperatures T_s [2]. The cathode spot model, which works well with cathodes having moderate thermophysical properties, predicts for refractory cathodes so small a plasma density that the temperature T_s cannot be supported by the outflow plasma energy to the electrode [1], [2]. This problem was overcome using a new *virtual cathode* model that takes in account that the electron density exceeds the ion density in the sheath adjacent to the cathode and the consequent negative space charge forms a potential minimum U_m with respect to the plasma potential and has a potential difference of ΔU with respect to the cathode (Fig. 8) [1], [2]. A lower electron emission current density j_e was obtained using the virtual plasma cathode model [2]. The electron beam relaxation zone with reduced electron emission current was considered. A solution was found, but the electron current fraction $s = j_e/j$ remained very large, more than 0.99 and, consequently, only a single large spot with current density $j > 10^6$ A/cm² was obtained [2]. However, slowly moving and steady-state spots with $j < 10^6$ A/cm² are

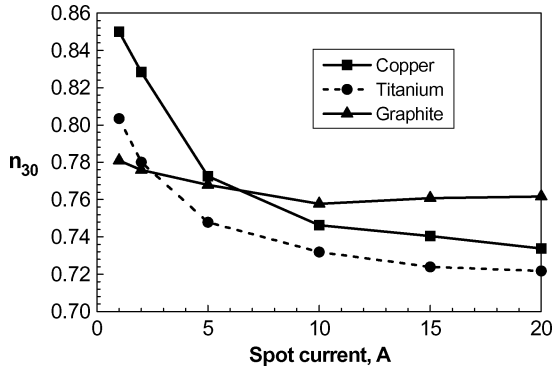


Fig. 7a. Heavy particle densities at the external boundary of the Knudsen layer n_3 normalized by the saturated density n_0 as functions of the spot current.

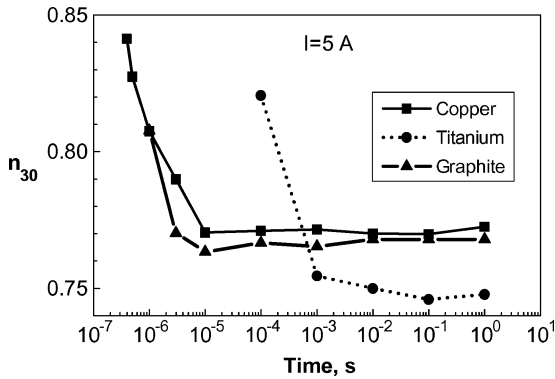


Fig. 7b. Time dependence of heavy particle densities at the external boundary of the Knudsen layer n_3 normalized by the saturated density n_0 .

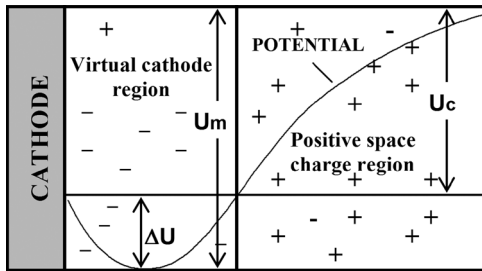


Fig. 8. Schematic presentation of the virtual cathode structure for a refractory cathode material.

observed on tungsten cathodes in vacuum arcs [8], [48]. Calculations [2], [44] also showed that with moderate cathode materials, the lower j is consistent with lower electron current fraction, e.g., $s < 0.8$.

Generally, when the virtual plasma cathode model was used, zero electric field at the plasma side of the sheath E_p was also assumed [49]. As a result, the ratio of emitted electron current density j_e to the incident ion current density j_i is proportional to the square root of the ion mass m to the electron mass m_e ratio, i.e. $j_e/j_i \sim (m/m_e)^{1/2}$ [49]. Thus, j_e is much larger than the ion current density j_i . A mathematical analysis of the sheath structure shows that with W cathode, in the near cathode region the ratio j_e/j_i will be lower if $E_p \neq 0$. This conclusion is consistent with the sheath-presheath models for the transition region between a negatively charged wall and a collision dominated plasma [50]–[53]. A model of virtual plasma cathode taking into account the nonzero electric field at the plasma sheath interface

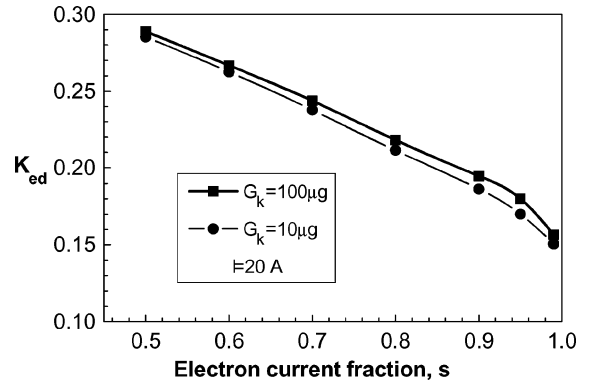


Fig. 9. Electric field at the sheath-plasma interface normalized by the ratio of the electron temperature to the Debye length as a function of the electron current fraction in the spot with W cathode erosion rate as parameter.

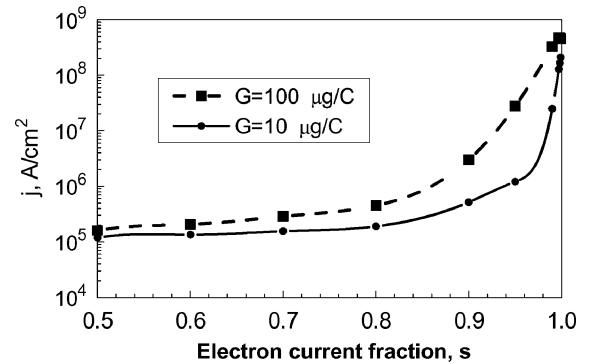


Fig. 10. Spot current density as function on electron current fraction in the spot with cathode erosion rate as parameter.

and electron beam relaxation zone in near cathode quasi-neutral plasma was developed for vacuum arc refractory cathodes [54]. The electric field E_p was calculated from Poisson's equation, taking into account the space charge from the ions, plasma electrons back-flowing towards the cathode and electrons emitted by the virtual cathode. A parameter K_{ed} was defined as the ratio of E_p to T_e/L_d , where L_d is the plasma Debye length. The dependence of K_{ed} was calculated as a function of s for $I = 20$ A and $U_c = 20$ V [5]. Fig. 9 shows that K_{ed} decreases with s and reaches about 0.1 for $s > 0.9$. For this condition, the spot current density j as function on s is presented in Fig. 10. It can be seen that j is about 10^5 A/cm² for $s < 0.9$.

Volatile Materials: The regular cathode spot models [2] also meet a discrepancy and cannot consistently explain the cathode spot operation on highly volatile cathode such as Hg . This discrepancy is explained below. According to the calculations, a relatively high plasma density of about $10^{19} - 10^{20}$ cm⁻³ is obtained from the saturated Hg pressure at low cathode temperatures, e.g., ~ 1000 °C. This plasma density is sufficient to balance the cathode energy. However, this cathode temperature is too low to provide sufficient electron emission. As a result, the plasma in the electron beam relaxation zone cannot be sufficiently heated, the plasma temperature is very low according to the plasma energy balance and the plasma cannot be regenerated. Thus, the traditional model for the volatile materials needed modification by adding a specific mechanism to control the plasma energy balance, current continuity and the mercury evaporation. Let us consider a double space sheath [55]

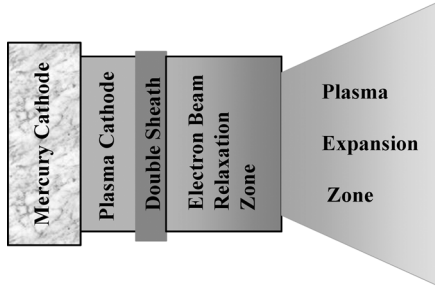


Fig. 11. Plasma layer structure with a plasma cathode and an electron beam relaxation zone near a Hg cathode.

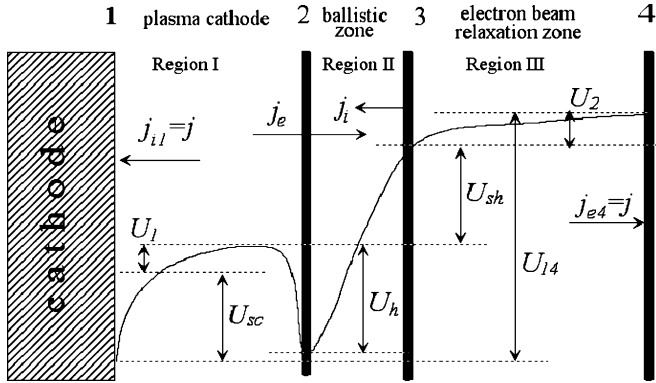


Fig. 12. Near cathode (mercury) schematic potential distribution in the cathode plasma region I (screening potential drop U_{sc}), in double sheath U_{sh} (region II) and in the electron beam relaxation zone (region III). U_1 and U_2 is the potential drop in the plasma regions I and III, respectively.

appeared in plasma volume and which is a transient layer between non emitted Hg cathode and conductive plasma.

Double Sheath Model: A model was proposed [55], in which the near-cathode region is modeled by two distinct regions, divided by a double space charge layer. Previously, a double layer in a high-voltage discharge with a low density of charged particles was observed experimentally [56]. Moreover, a double layer also appears over a considerable range of the particle densities when sharp changes of the discharge channel cross section occur [57] or in plasma configurations with divergent magnetic field [58]–[61]. The principle cathode plasma structure in the case of Hg is presented schematically in Fig. 11. The schematic potential distribution in the different plasma regions is shown in Fig. 12. According to the model [55], the plasma region I directly contacts the cathode surface (boundary 1) and in this region a screening potential drop U_{sc} is formed. The plasma region I shares boundary 2 with the double sheath layer (region II). Electrons are created in region I by electron impact, and boundary 2 thus serves as a plasma cathode for the rest of the discharge, while current continuity is maintained at boundary 1 mostly by the ion current. Thus, there is no requirement for the cathode surface to emit an electron current equal to the circuit current—the electrons are generated by the plasma cathode, similar to what occurs in the cathode region of a glow discharge.

Region II (ballistic zone) is a collisionless space charge double-layer having a relatively large potential drop U_{sh} . Generally, the thickness of the double layer is of the order of the Debye length. Region II borders the external plasma (region III)

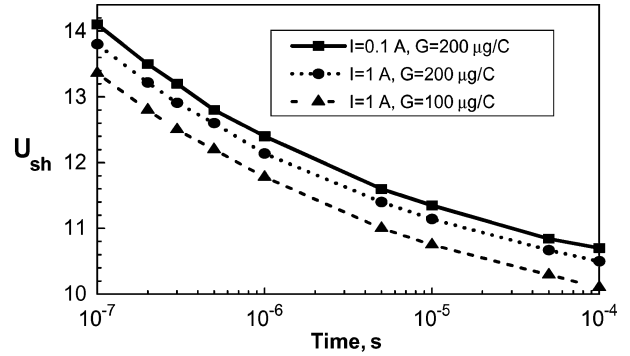


Fig. 13. Time dependence of sheath potential drop for mercury cathode.

which extends to boundary 4 in the anode direction. Its length is the *relaxation length of the electron beam* emitted from region I. Both electrons emitted from region I in the direction of the anode, and ions extracted from region III (see Fig. 12) pass through the double-layer (region II) on the way to their respective destinations, and are accelerated by the potential drop in the double layer. The additional energy imparted to the plasma particles on their way to region I is critical in providing the power that ultimately is necessary for ionization, and hence producing the necessary electron flux in region I. Excited atoms flowing into the first plasma region play also an important role in its energy balance, as does the outflow of the atoms from region III. The excited atoms at the metastable level should be taken in account for produce step ionization of the mercury atoms [55].

A 1-D system of equations describing current continuity and energy conservation were formulated and solved for the above model [55]. Two types of time-dependent solutions were found, with characteristics times of 0.1–1 μs and 100 μs , respectively. These times correspond to the experimentally observed spot life times for the transitional and fundamental arc forms, respectively observed by Kesaev [10].

The potential drop in the plasma regions (Fig. 12) U_1 and U_2 , typically <0.5 V, are small in comparison to the double sheath potential drop U_{sh} (10–15 V). Fig. 13 shows that U_{sh} decreases with spot life time and depends weakly on the spot current, if the cathode erosion coefficient is constant. The calculation shows that U_{sh} can be small (~ 10 V) in accordance with the measurements of the arc voltage with Hg cathode [10]. The length of the first plasma region is calculated to be 10 μm , which is approximately equal to the experimentally observed dark space in the Hg vacuum arc [10]. Acceleration of electrons from the first plasma region through the layer with potential drop $U_{sh} + U_h$ explains the observation of fast electrons with energy exceeded the measured arc voltage [10].

VII. SUMMARY AND DISCUSSION

Strong vapor density and temperature jumps appear near vaporized walls due to intensive heating. The back flux to the wall is generated in a length of few mean free paths in the nonequilibrium (Knudsen) layer, adjacent to the vaporized wall. When only atom collisions produce back flux, the vapor flows with sound velocity v_{sn} at the external boundary of the Knudsen layer. This occurs in moderate power laser-matter interactions

[6]. Another case is for electrode vaporization into an adjacent current-carrying discharge plasma. Since the atoms are ionized and an additional energy is dissipated in the plasma volume, the plasma flows with a subsonic velocity at the external boundary of the Knudsen layer. We named these as the free flow regime ($v = v_{sn}$) and the impeded (nonfree) flow regime ($v < v_{sn}$) [35], [36].

In the vacuum arc cathode region, electron emission plays an important role in supporting the current continuity of the discharge. In particular, the relaxation zone of a highly energetic electron emission beam is much larger than mean free paths of the heavy particles and plasma electrons. This fact allows understanding the plasma phenomena (vapor ionization, current, mass and energy transfer) by a plasma hydrodynamic treatment using the plasma parameters at the Knudsen layer as boundary conditions. A self-consistent solution of the plasma flow in the Knudsen layer and in the hydrodynamic region shows a number of effects in a vacuum arc cathode ablation. Below we summarize the main results.

- 1) In vacuum arc cathode spots, the mass flow is significantly impeded and the normalized velocity $b_3 \ll 1$. In the calculated region of I and t for the vacuum arc cathode spot, the heavy particle density at the external boundary of Knudsen layer to the saturated density ratio $n_3/n_0 = 0.72 - 85$ is significantly larger than in the case of free laser evaporation in vacuum, where it is $n_3/n_0 = 0.3$ [6], [31]. This means that the Knudsen layer structure problem in high current discharges is different from laser metal evaporation. The difference is due to different vapor generation conditions. Indeed, in the case of laser action ($10^4 - 10^5$ W/cm²), the heat flux to the target is determined by an external heat source (laser power) which is independent of the extracted vapor intensity (except the effect of "plasma shielding" which described by an absorption coefficient in case of high intensity laser irradiation, $\geq 10^6$ W/cm², when the absorbed energy can influence on the plasma expansion [25]). Therefore, the vapor freely expands into vacuum at the sound velocity.

Another case includes electrode vaporization in vacuum arc spots and ablative accelerators, unipolar arc in tokamaks, capillary discharges, etc. In those cases, the heat flux to the wall is determined by parameters of the generated plasma, i.e., the evaporation phenomenon is coupled with the adjacent plasma. For example, in the cathode spot, the ion flux to the cathode, which serves as the primary energy source for the cathode, depends on the cathode evaporation rate, vapor velocity, and its ionization. A large fraction of the returning mass flux to the cathode is a result of the cathode erosion products flow in a condition when the plasma and cathode heating are supported self-consistently. Thus, the plasma flow velocity depends on the energy dissipation in the electrode body and in the plasma, and is controlled by condition (certain level of plasma density and plasma temperature) supported the cathode spot operation. Therefore, the plasma flow is impeded, the plasma velocity at the external boundary of Knudsen layer is less than the sound velocity, and the cathode vapor expansion is impeded. As a result, the rate

of cathode mass loss is lower than by free-flow regime of evaporation in vacuum supported by laser radiation. This result has experimental evidence explaining the transition of instable fast moving spot type (flow impeded only by own spot plasma) to type of slow relatively stable spot when the background pressure increase (plasma expansion from the spot is limited by the external gas pressure) and understand the arc voltage fluctuation at low (threshold) current arc in vacuum [1], [2], [5].

- 2) The electron emission can be considered as electron evaporation from the heated cathode. As a result, the jumps of electron density and temperature are not originated similarly as the jump of the heavy particle because the beam electrons have the following characteristics: a) the electrons are charged particle moving in an electrical field and b) the accelerated electrons move in a zone with an addition electron source due to ionization. Therefore, the plasma energy balance changes due to electron emission energy dissipation in the quasi-neutral plasma region which is the electron relaxation zone. The beam electron relaxation zone is analogues to an electron beam Knudsen layer. Electron beam relaxation is an important phenomenon which determines the regeneration mechanism of the plasma slow electrons and ions supporting the vacuum arc operation.
- 3) The mechanism of current continuity and the structure of wall plasma transition depend on the physical properties of the cathode materials. This dependence is determined by the relation between rates of electron and atom evaporation. The structure of the wall to plasma transition region provides the conditions for electron transport in the cathode plasma region. When a relatively large ion current to the cathode is generated the large electric field at the cathode surface occurs. This electric field enhanced the cathode electron emission and supports the cathode heating by ion bombardment at a level for sufficient cathode evaporation. This mechanism occurs with a wide region of cathode materials with intermediate physical properties. Previously, such an approach was also used for cathode materials with violently different physical properties but in calculations with arbitrary parameters [5], [10]. However, the closed system of equations for model based on a high electric field at the cathode surface cannot be solved for volatile (e.g., Hg) and refractory (e.g., W) cathode materials.

In the volatile case, the electron emission is practically negligible in comparison to the rate of evaporation and, therefore, a model with a double sheath and a plasma cathode was proposed [55] to explain the nature of current continuity in the cathode-plasma transition region near the cathode. The calculated low cathode potential drop, which explains the observed cathode voltage of 9–10 V, is an important feature of the double sheath model for the Hg cathode.

Just the opposite is the case of a refractory cathode for which the rate of atom evaporation is negligible compared to the high rate of electron evaporation, and therefore a vanishingly small ion current was obtained in frame of the traditional cathode spot model [1], [2], [44]. Therefore, a virtual cathode model was de-

vised [54] which allows sufficient reduction of the large electron emission flux. The important point of the virtual cathode model is that the electric field in vicinity of the cathode surface in the sheath is typically zero while *at the sheath-plasma interface the electric field is significant*. This sheath structure supports a relatively large ion current fraction which is necessary for self-consistent W cathode spot operation. The mentioned electric field is calculated to be much smaller than the field determined by the ratio of electron temperature to the Debye length. This electric field is necessary for supporting a relatively low spot current density on tungsten cathodes, as observed experimentally.

In summary, it should be emphasized that the material vaporization in the current-carrying self-sustained systems consists of several complicated phenomena including the mass flow from the target in the Knudsen layer, the plasma energy dissipation in the ionization and expansion regions and the plasma-electrode transition layer. The aforementioned typical structures are different for materials with different thermal properties.

ACKNOWLEDGMENT

The author would like to thank to Prof. R. L. Boxman for useful comments.

REFERENCES

- [1] I. I. Beilis, "State of the theory of vacuum arcs," *IEEE Trans. Plasma Sci.*, vol. 29, no. 5, pp. 657–670, Oct. 2001.
- [2] ———, "Theoretical modeling of cathode spot phenomena," in *Vac. Arc Sci. Technol.* R. L. Boxman, P. Martin, and D. Sanders, Eds., Park Ridge, NJ: Noyes, 1995.
- [3] R. L. Burton and P. J. Turchi, "Pulsed plasma thruster," *J. Propulsion Power*, vol. 14, no. 5, pp. 716–735, 1998.
- [4] G. M. McCracken, "A review of the experimental evidence for arcing and sputtering in tokamaks," *J. Nucl. Materials*, vol. 93/94, pp. 3–16, 1980.
- [5] R. L. Boxman, P. Martin, and D. Sanders, Eds., *Vacuum Arc Science and Technology*. Park Ridge, NJ: Noyes, 1995.
- [6] S. I. Anisimov, Y. A. Imas, G. S. Romanov, and Y. V. Khodyko, *Action of High-Power Radiation on Metals*. Springfield, VA: Nat. Tech. Inf. Serv., 1971.
- [7] I. I. Beilis, "Anode spot vacuum arc model: Graphite anode," *IEEE Trans. Compon. Packag. Technol.*, vol. 23, no. 2, pp. 334–340, Jun. 2000.
- [8] V. I. Rakhovsky, "Experimental study of the dynamics of cathode spots development," *IEEE Trans. Plasma Sci.*, vol. 4, pp. 87–102, 1976.
- [9] B. Juttner, "Cathode spots of electrical arcs," *J. Phys. D, Appl. Phys.*, vol. 34, pp. R103–123, 2001.
- [10] I. G. Kesaev, *Cathode Processes in Electric Arcs* (in Russian). Moscow, USSR: Nauka, 1968.
- [11] S. Cuperman, D. Zoler, and J. Ashkenazy, "Analysis of plasma critical flow in a combined discharge capillary-ablative pipe system," *Plasma Sources Sci. Technol.*, vol. 3, pp. 593–601, 1994.
- [12] S. V. Kukhlevsky, J. Kaiser, O. Samek, M. Liska, and J. Erostryak, "Stark spectroscopy measurements of electron density of ablative discharges in Teflon-(CF₂)_n capillaries," *J. Phys. D, Appl. Phys.*, vol. 33, pp. 1090–1092, 2000.
- [13] M. Bourham, O. Hankis, O. Auciello, J. Stock, and B. Wenring, "Vapor shielding and erosion of surface exposed a high heat load in an electrothermal accelerator," *IEEE Trans. Plasma Sci.*, vol. 17, pp. 386–391, 1989.
- [14] I. I. Beilis and V. E. Ostashow, "Model for a high-current discharge moving between parallel electrodes," *High Temp.*, vol. 27, no. 6, pp. 817–821, 1989.
- [15] D. A. Weeks, W. F. Wedon, and R. C. Zowarka, "Plasma-armature railgun launcher simulations," *IEEE Trans. Plasma Sci.*, vol. 17, no. 3, pp. 403–408, Jun. 1989.
- [16] C. B. Ruchti and L. Niemeyer, "Ablation controlled arcs," *IEEE Trans. Plasma Sci.*, vol. 14, no. 4, pp. 423–434, Aug. 1986.
- [17] P. J. Turchi, "Directions for improving PPT performance," in *Proc. 25th Int. Electric Propulsion Conf. Electric Rocket Propulsion Soc.*, Worthington, OH, 1998, vol. 1, pp. 251–258.
- [18] J. Ashkenazy and D. Zoler, "Analysis of plasma critical flow in ablative discharge capillaries with a non-constant cross-section," *J. Plasma Phys.*, vol. 53, no. 3, pp. 267–276, 1995.
- [19] G. E. Rolader and J. H. Batten, "Thermodynamic and electrical properties of railgun plasma armatures," *IEEE Trans. Plasma Sci.*, vol. 17, no. 3, pp. 439–445, Jun. 1989.
- [20] I. I. Beilis, "The near-cathode region of contracted discharge at the metal electrode of MHD generator," *High Temp.*, vol. 15, no. 6, pp. 1269–1275, 1977.
- [21] A. E. Robson and P. C. Thoneman, "An arc maintained on an isolated metal plate exposed to a plasma," in *Proc. Phys. Soc.*, 1959, vol. 73, pp. 508–510.
- [22] V. Philipps, U. Samm, M. Tokar, B. Unterberg, A. Pospieszczyk, and B. Schweer, "Evidence of hot spot formation on carbon limiters due to thermal electron emission," *Nucl. Fusion*, vol. 33, no. 6, pp. 953–961, 1993.
- [23] I. G. Levchenko, A. U. Voloshko, M. Keidar, and I. I. Beilis, "Unipolar arc behavior in high frequency fields," *IEEE Trans. Plasma Sci.*, vol. 31, no. 1, pp. 137–141, Jan. 2003.
- [24] M. Laux, W. Schneider, B. Juttner, S. Linding, M. Mayer, M. Balden, I. I. Beilis, and B. Djakov, "Modification of tungsten layers by arcing," *J. Nucl. Mater.*, vol. 337–339, pp. 1019–1023, 2005.
- [25] A. Bogaerts, Z. Chen, R. Gijbels, and A. Vertes, "Laser ablation for analytical sampling: What can we learn from modeling?," *Spectrochimica Acta, Part B*, vol. 58, pp. 1867–1893, 2003.
- [26] Z. Chen and A. Bogaerts, "Laser ablation of Cu and plume expansion into 1 atm ambient gas," *J. Appl. Phys.*, vol. 97, p. 063305, 2005.
- [27] S. I. Anisimov and V. Khokhlov, *Instabilities in Laser-Matter Interaction*. Boca Raton, FL: CRC, 1995.
- [28] I. Langmuir, "The vapor pressure of metallic tungsten," *Phys. Rev.*, vol. II, no. 5, pp. 329–342, 1913.
- [29] M. Knudsen, "Die maximale verdampfungsgeschwindigkeit des quecksilbers," *Ann. Phys. Chem.*, vol. 47, pp. 697–708, 1915.
- [30] P. L. Bhatnagar, E. P. Cross, and M. Krook, "A model for collision processes in gases. I. Small amplitude processes in charged and neutral one-component systems," *Phys. Rev.*, vol. 94, no. 3, pp. 511–525, 1954.
- [31] S. I. Anisimov, "Vaporization of metal absorbing laser radiation," *JETP*, vol. 37, no. 1, pp. 182–183, 1968.
- [32] H. M. Mott-Smith, "The solution of the Boltzmann equation for a shock wave," *Phys. Rev.*, vol. 2, no. 6, pp. 885–892, 1951.
- [33] O. Knake and I. N. Stranski, "Mechanism of vaporization," *Progress in Metal Physics*, vol. 6, pp. 181–235, 1956.
- [34] J. Fisher, "Distribution of pure vapor between two parallel plates under the influence of strong evaporation and condensation," *Phys. Fluids*, vol. 19, no. 9, pp. 1305–1311, 1976.
- [35] I. I. Beilis, "On the theory of erosion processes in the cathode region of an arc discharge," *Sov. Phys. Doklady*, vol. 27, pp. 150–153, 1982.
- [36] ———, "Cathode arc plasma flow in a Knudsen layer," *High Temp.*, vol. 24, pp. 319–325, 1986.
- [37] C. J. Knight, "Theoretical modeling of rapid surface vaporization with back pressures," *AIAA J.*, vol. 17, no. 5, pp. 519–523, 1979.
- [38] R. L. Baker, "Kinetically controlled vaporization of a polyatomic gas," *AIAA J.*, vol. 29, no. 3, pp. 471–473, 1991.
- [39] I. I. Beilis, "Parameters of kinetic layer of arc discharge cathode region," *IEEE Trans. Plasma Sci.*, vol. PS-13, no. 5, pp. 288–290, 1985.
- [40] M. Keidar, I. D. Boyd, and I. I. Beilis, "On the model of Teflon ablation in an ablation-controlled discharge," *J. Phys. D, Appl. Phys.*, vol. 34, pp. 1675–1677, 2001.
- [41] M. Keidar, J. Fan, I. D. Boyd, and I. I. Beilis, "Vaporization of heated materials into discharge plasmas," *J. Appl. Phys.*, vol. 89, no. 6, pp. 3095–3098, 2001.
- [42] M. Keidar, I. D. Boyd, and I. I. Beilis, "Ionization and ablation phenomena in an ablative plasma accelerator," *J. Appl. Phys.*, vol. 96, no. 10, pp. 5420–5428, 2004.
- [43] ———, "A model of an electrothermal pulsed plasma thruster," *J. Propulsion Power*, vol. 19, no. 3, pp. 424–430, 2003.
- [44] I. I. Beilis, "Analysis of the cathode spots in a vacuum arc," *Sov. Phys. Tech. Phys.*, vol. 19, no. 2, pp. 251–260, 1974.
- [45] L. A. Arzimovich and R. Z. Sagdeev, *Physics for Physicists*. : Atomizdat, 1979, M.
- [46] I. I. Beilis, G. A. Lyubimov, and V. I. Rakhovsky, "Diffusion model of the near cathode region of a high-current arc discharge," *Sov. Phys. Doklady*, vol. 17, pp. 225–228, 1972.

- [47] L. N. Dobretzov and M. V. Homoyunova, *Emission Electronics*. Moscow, USSR: Nauka, 1966.
- [48] W. Finkelnburg and H. Maecker, "Electrische bogen und thermishes plasma," in *Handbuch der Physik*, vol. XXII, pp. 254–444.
- [49] I. Langmuir, "The interaction of electron and positive ion space charges in cathode sheaths," *Phys. Rev.*, vol. 33, no. 6, pp. 954–989, 1929.
- [50] K. U. Reimann, "The influence of collisions on the plasma-sheath transition," *Phys. Plasmas*, vol. 4, no. 11, pp. 4158–4166, 1997.
- [51] I. I. Beilis and M. Keidar, "Sheath and presheath structure in the plasma wall-transition layer in an oblique magnetic field," *Phys. Plasmas*, vol. 5, no. 5, pp. 1545–1553, 1998.
- [52] N. Sternberg and V. Godyak, "On asymptotic matching and the sheath edge," *IEEE Trans. Plasma Sci.*, vol. 31, no. 4, pp. 665–677, Aug. 2003.
- [53] M. Keidar and I. I. Beilis, "Transition from plasma to space-charge sheath near the electrode in electrical discharges," *IEEE Trans. Plasma Sci.*, vol. 33, no. 5, pp. 1481–1486, Oct. 2005.
- [54] I. I. Beilis, "A mechanism for small electron current fraction in a vacuum arc cathode spot on a refractory cathode," *Appl. Phys. Lett.*, vol. 84, no. 8, pp. 1269–1271, 2004.
- [55] I. I. Beilis, "Current continuity and instability of the mercury vacuum arc cathode spot," *IEEE Trans. Plasma Sci.*, vol. 24, no. 4, pp. 1259–1271, Aug. 1996.
- [56] E. I. Lutsenko, N. D. Sereda, and L. M. Kontsevoi, "Investigation of the charge volume sheath creation in plasmas," *Sov. J. Plasma Phys.*, vol. 2, no. 1, p. 39, 1976.
- [57] J. G. Andrews and J. E. Allen, "Theory of a double sheath between two plasmas," in *Proc. R. Soc.*, 1971, vol. A320, pp. 459–472.
- [58] X. Sun, A. M. Keesee, C. Biloiu, and E. E. Scime, "Observations of ion-beam formation in a current-free double layer," *Phys. Rev Lett.*, vol. 95, p. 025004, 2005.
- [59] S. A. Cohen, N. S. Siefert, S. Stange, R. F. Boivin, E. E. Scime, and F. M. Levinton, "Ion acceleration in plasmas emerging from a helicon-heated magnetic-mirror device," *Phys. Plasmas*, vol. 10, no. 6, pp. 2593–2598, 2003.
- [60] X. Sun, S. A. Cohen, E. E. Scime, and M. Miah, "On-axis parallel ion speeds near mechanical and magnetic apertures in a helicon plasma device," *Phys. Plasmas*, vol. 12, p. 103509, 2005.
- [61] C. Charles and R. Boswell, "Current-free double-layer formation in a high-density helicon discharge," *Appl. Phys. Lett.*, vol. 82, no. 9, pp. 1356–1358, 2003.



Isak I. Beilis (M'97–SM'00) received the M.Sc. degree from Moscow Institute for Steel and Alloys, Moscow, U.S.S.R., in 1966, the Ph.D. degree and degree of Doctor of Physical and Mathematical Sciences from the U.S.S.R. Academy of Science, St. Petersburg, Russia, in 1973 and 1990, respectively.

From 1969 to 1991, he was with Institute for High Temperatures (IVTAN), Moscow, also holding a position of Visiting Scientist in the Institute of Mechanics of the Moscow Lomonosov University.

Since January 1992, he has been continuing his investigations at the Faculty of Engineering at Tel Aviv University, Tel Aviv, Israel. His research is concerned with the electrical discharges in vacuum interrupters, MHD-generators, plasma accelerators, arc cathode and anode spots, vacuum arc plasma jet expansion in magnetic fields, plasma-wall transition, kinetic of condensed material vaporization into current carrying plasma, dusty plasma transport in ducts, macroparticle charging phenomena, hot electrode vacuum arc-physics and its application in a coatings. He is co-author of the books "*MHD Energy Conversion.—Physical and Technical Aspects*" (Nauka, 1982), and "*Handbook of Vacuum Arc Science and Technology*" (Noyes, 1995).